Parametric motion of energy levels: Curvature distribution

P. Gaspard
Service de Chimie-Physique, Université Libre de Bruxelles, Campus Plaine, Code Postal 231, B-1050 Brussels, Belgium

S. A. Rice
Department of Chemistry and The James Franck Institute, The University of Chicago, Chicago, Illinois 60637

H. J. Mikeska
Institut für Theoretische Physik, Universität Hannover, Hannover 3000, Federal Republic of Germany

K. Nakamura
Department of Physics, Fukuoka Institute of Technology, Higashi-ku, Fukuoka 811-02, Japan
(Received 26 February 1990)

We study the statistical properties of the distortions of irregular energy spectra when a perturbation parameter is varied; for example, the strength of an external field acting on the bounded quantum system. Three kinds of generalized Calogero-Moser (GCM) classical Hamiltonians are shown to rule the parametric motion of the energy levels in orthogonal, unitary, and symplectic systems. Using these GCM Hamiltonians, we construct a Newtonian theory of ensembles where irregular spectra are correlated with the properties of infinite gases of GCM particles. In this dynamical approach, the results of random matrix theory are recovered. Furthermore, we are able to study parametric properties of irregular spectra such as the level curvature defined by the second derivative of a level energy with respect to the perturbation parameter. We prove that the level curvature density of the orthogonal, unitary, and symplectic systems decreases, respectively, as $|K|^{-3}$, $|K|^{-4}$, and $|K|^{-6}$ for large curvature $|K|$. We present numerical results supporting our theoretical analysis and suggesting the universality of the curvature distribution. The relationship of the curvature distribution to the spacing distribution, as well as the possible experimental observation of the curvature distribution, is discussed.

I. INTRODUCTION

Several recent experiments have been concerned with the motion of the energy levels of bounded quantum systems when a parameter is varied. The observed systems are, for instance, atoms or molecules in an external static electric or magnetic field.[1,2]

In the absence of the perturbation the Hilbert space of the quantum system is often separated into one-dimensional linear manifolds labeled by the quantum numbers of the constants of motion. However, these manifolds become intermixed when the perturbation is switched on, and categorization of the energy levels with a complete set of constants of motion is not possible. Then, the energy spectrum is characterized by a multitude of avoided-level crossings or repulsions of adjacent energy levels. (If the perturbed system retains some symmetries, the desymmetrized spectra should be considered so as to suppress the true crossings.) These avoided crossings lead to an irregular spectrum whose description requires a statistical study of the energy levels.[3]

Irregular spectra have been the subject of many recent studies, the results of which show that they usually arise in classically nonintegrable and chaotic systems.[4] Such spectra are characterized by several statistical quantities: the spacing distribution, the static correlation function, the spectral rigidity, all of which are suggested by random matrix theory[5] and which have been measured experimentally.[6] The studies cited concern systems where the perturbation parameter is fixed once and for all.

However, there have been only a few studies of the parametric properties of irregular spectra such as can be observed in diagrams where the energy spectrum is plotted versus the perturbation parameter.[7,8] Several authors have used the second difference of the eigenvalues with respect to the perturbation parameter τ,[3,7]

$$\Delta^2 E_i \equiv E_i(\tau+\Delta\tau)-2E_i(\tau)+E_i(\tau-\Delta\tau) , \tag{1.1}$$

to characterize the effect of classical nonintegrability on the corresponding quantum spectrum; in particular, for the Hénon-Heiles system. We shall call this parametric quantity the curvature, after taking the appropriate limit:

$$K_i \equiv \ddot{E}_i(\tau) = \lim_{\Delta\tau\to 0} \frac{\Delta^2 E_i}{\Delta\tau^2} . \tag{1.2}$$

In fact, the curvature in (1.2) takes particularly large values for a pair of levels at avoided crossings and constitutes a nice hallmark of the quantum analog of classical nonintegrability. This paper develops a statistical theory of such parametric properties for irregular spectra in order to reveal general laws of wide applicability. In this approach, we shall derive the tail of the probability distribution of the curvature and give arguments suggesting its

universality.[9] The statistical theory we develop is a generalization of the random matrix theory to systems depending on a perturbation parameter. Accordingly, we recover from our analysis the results of random matrix theory.[5]

In Sec. II we define the curvature distribution and we give one example of it. In Sec. III we display the equations of motion of the eigenvalues $\{E_i(\tau)\}$ when the parameter τ is varied. In Sec. IV we define the ensembles of our statistical theory. We confirm that the spacing distributions for our ensembles are the universal distributions of Mehta, Gaudin, and Dyson[10–14] in Sec. V. The tail of the curvature distribution is calculated in Sec. VI. We present numerical results supporting our theory in Sec. VII and discuss our conclusions in Sec. VIII.

II. CURVATURE DISTRIBUTION

A. Definition

We consider bounded quantum systems that are either autonomous or periodically driven. The spectrum is then represented, respectively, by the eigenvalues $\{E_i(\tau)\}$ either of the energy or of the quasienergy in Floquet's theory.[15] If a finite set $\mathcal{J}$ of eigenvalues is chosen, the frequency distribution function of the curvature is defined by

$$\mathcal{F}(K;\mathcal{J}) \equiv \frac{1}{\mathcal{N}\mathcal{J}} \mathcal{N}\{E_i(\tau) \text{ in } \mathcal{J} \text{ such that } \ddot{E}_i(\tau) < K\} , \tag{2.1}$$

where $\mathcal{N}$ denotes the number of elements in the corresponding set. For an autonomous system, $\mathcal{J}$ contains all the energy levels below some maximum, $E_i(\tau) < E_{\max}$. Because the number of eigenvalues is finite, (2.1) is a step function which, in general, depends on the parameter τ. A smooth distribution will be obtained in the classical limit where the number of eigenvalues in $\mathcal{J}$ becomes infinite,

$$\mathcal{F}(K) = \lim_{\mathcal{N}\mathcal{J}\to\infty} \mathcal{F}(K;\mathcal{J}) . \tag{2.2}$$

For autonomous systems that are bounded at any energy, it is sufficient to take the limit $E_{\max} \to +\infty$. In systems with a forcing period T, the quasienergy is always contained in $[0, 2\pi\hbar/T[$,[15] so that we must consider other possible classical limits where the number of quasienergy eigenstates increases indefinitely (see below).

The density of the curvature distribution is then

$$\mathcal{P}(K) \equiv \frac{d\mathcal{F}}{dK} , \tag{2.3}$$

when the distribution is smooth enough.

The definition (2.1) is valid when the spectrum is uniform or assimilable. If such is not the case, the curvature must be rescaled according to

$$\ddot{E}_i \frac{\langle E_{i+1} - E_i \rangle_{\rm sl}}{\langle (\dot{E}_i)^2 \rangle_{\rm sl}} , \tag{2.4}$$

before calculating the frequency distribution function. The brackets $\langle\ \rangle_{\rm sl}$ define a semilocal average over a range of energy where the spectrum is reasonably uniform. The theoretical justification for this scaling will be given at the end of Sec. VI. Let us note here that (2.4) is, as required, dimensionless.

B. Example

We illustrate our definition of the curvature distribution with the periodically kicked spin system given by the following single-spin Hamiltonian:[16,17]

$$\hat{H} = A(\hat{S}_z)^2 - \mu B \hat{S}_x \sum_{n=-\infty}^{+\infty} \delta(t - nT) , \tag{2.5}$$

where $A > 0$ is an easy-plane anisotropy, $B > 0$ is the external magnetic field along the x axis, and μ is the Bohr magneton. The quantum spin operators $\hat{\mathbf{S}} = (\hat{S}_x, \hat{S}_y, \hat{S}_z)$ satisfy the usual angular momentum commutation relations

$$[\hat{S}_x, \hat{S}_y] = i\hbar\hat{S}_z \quad \text{with } \hat{\mathbf{S}}^2 = \hbar^2 s(s+1)\hat{I} , \tag{2.6}$$

and they act on a $(2s+1)$-dimensional Hilbert space. The classical limit is obtained for $s \to +\infty$. The role of the perturbation parameter is, in this case, played by the external magnetic field B. We assign the other parameters the values $A = 1$, $\mu = 1$, $T = 2\pi$, and $\hbar = 1$.

The one-period propagator is the unitary matrix

$$\hat{U} = e^{(\iota/\hbar)\mu B \hat{S}_x} e^{-(\iota/\hbar) T A (\hat{S}_z)^2} = \sum_{m=1}^{2s+1} |m\rangle e^{-(\iota/\hbar) T E_m} \langle m| , \tag{2.7}$$

with $2s+1$ eigenvalues on the unit circle giving the quasienergies.

Noting the invariance of $\hat{H}$ under the transformation $\hat{S}_z \to -\hat{S}_z$, however, we have decomposed the manifold into odd- and even-parity parts. We have calculated the quasienergies corresponding to (2.7) numerically in each part of the manifold. Only the results for the even-parity part are given in Figs. 1–5. Figure 1 shows how they vary with the external magnetic field for a spin $s = 16$. The histograms of the spacings $\{E_{m+1} - E_m\}$ are calculated from diagrams like Fig. 1 and are shown in Fig. 2 for $s = 64$ and in Fig. 4 for the larger spin $s = 160$. The corresponding histograms of the curvatures are shown in Fig. 3 for $s = 64$ and in Fig. 5 for $s = 160$. The curvatures $\{\Delta^2 E_m / \Delta B^2\}$ were computed using the discrete form (1.1) of the second-order derivative, with $\Delta B = 10^{-4}$. The size of ΔB limits the values where the curvature is confidently calculated to the range $|K| \le K_c$ with $K_c \sim 10^3$. This range can be increased using smaller values for ΔB. Another possible method is described in Sec. VII.

In the absence of a magnetic field, the spectrum is characterized by the absence of systematic repulsion between the levels and by a weak curvature [cf. Figs. 2(a), 3(a), 4(a), and 5(a)]. Once the magnetic field is switched on, rare but extremely narrow avoided-level crossings appear with correspondingly large curvatures. Thereafter, the repulsion phenomenon dominates the spectrum and

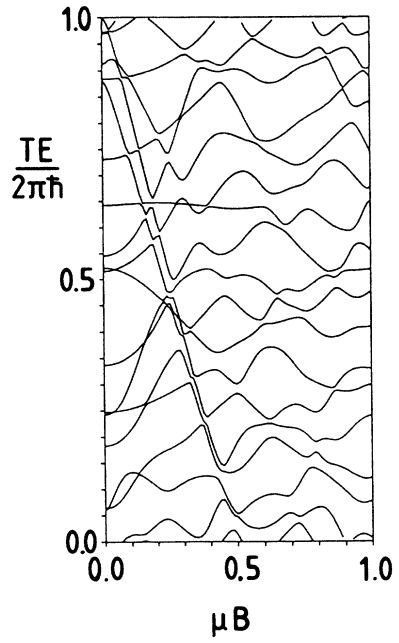

FIG. 1. Quasienergy spectrum vs the external magnetic field B for the pulsed-quantum spin system of Hamiltonian (2.5) with spin magnitude $s=16$, and parameter values $A=\mu=\hbar=1$ and $T=2\pi$. Only the even parity manifold of dimension 17 is depicted in the fundamental zone ($0\leq E<1$).

the spacing density vanishes near zero [cf. Figs. 2(b), 2(c), 4(b), and 4(c)]. Simultaneously, the curvature density is broadened, reflecting the appearance of avoided crossings [cf. Figs. 3(b), 3(c), 5(b), and 5(c)].

This observation suggests that the curvature distribution is intimately related to the spacing distribution. The smaller the spacing between two levels, the larger the curvature in absolute value. We thus expect that the behavior of the spacing density near zero determines the tail of the curvature density at large values of the curvature.

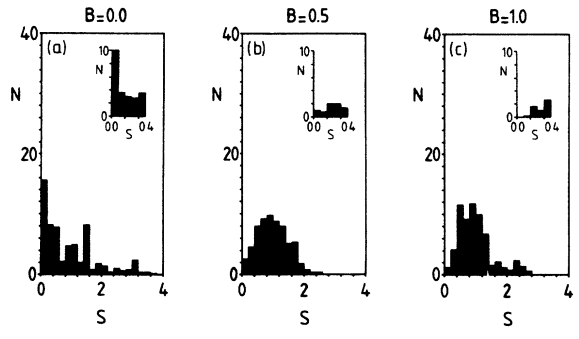

FIG. 2. Density of the level spacing of the same system as in Fig. 1 but with spin magnitude $s=64$ at different magnetic-field strengths: (a) $B=0.0$, (b) $B=0.5$, (c) $B=1.0$. The cells of the histogram have a size $\Delta B=0.2$. Inset: magnification of the histogram near zero spacing but with fivefold finer cells.

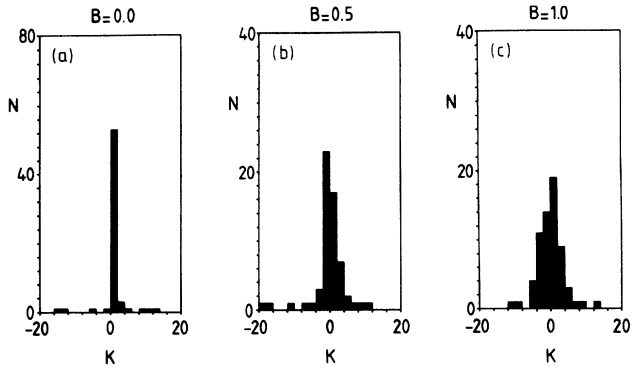

FIG. 3. Density of the level curvature for the same system as in Fig. 2 at different magnetic-field strengths: (a) $B=0.0$, (b) $B=0.5$, (c) $B=1.0$. Note the scale difference in ordinates between (a) and (b), (c).

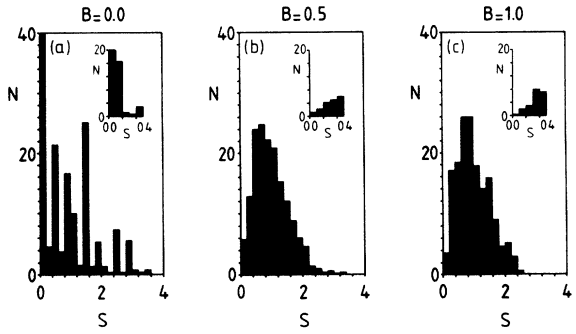

FIG. 4. Density of the level spacing for the same system as in Figs. 1 and 2 but now with spin magnitude $s=160$ at different magnetic-field strengths: (a) $B=0.0$, (b) $B=0.5$, (c) $B=1.0$. Inset: fivefold refinement of the histogram near zero spacing. The statistics are now improved. Comparing Figs. 2 and 4, the histogram is seen not to converge to a smooth density in the absence of external field (a), while it does so in the case when the field is switched on [(b) and (c)]. Note the vanishing of the spacing density near zero spacing showing the level repulsion phenomenon when the external magnetic field is switched on.

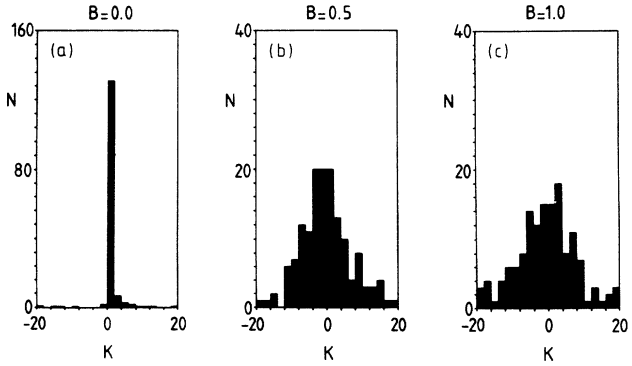

FIG. 5. Density of the level curvature for the same system as in Fig. 4. Note the broadening of the curvature density in the presence of the magnetic field together with the same notice as in Fig. 3.

III. PARAMETRIC MOTION OF THE LEVELS

In the following, we shall restrict ourselves to autonomous systems; how the following theory can be extended to periodically kicked systems will be explained in Sec. VIII. We shall consider systems which depend linearly on the parameter τ with a Hamiltonian operator

$$\hat{H}(\tau)=\hat{H}_0+\tau\hat{V} \ , \tag{3.1}$$

which is Hermitian because its eigenvalues must always be real. Many physical phenomena can be described by a Hamiltonian of this form, including the Stark effect and the linear Zeeman effect.

We assume that the Hamiltonian operator (3.1) acts in the Hilbert space of fixed quantum numbers corresponding to the few remaining constants of motion, e.g., the total angular momentum or the parity, when they exist. In the absence of further constants of motion which would diagonalize the energy operator (3.1), the diagonalization can be carried out by an orthogonal, a unitary, or a symplectic transformation, according to the three universality classes of Dyson.[13] The physical systems contained in each of these classes are described in Porter's review.[14] The matrix elements of the energy operator are then real, complex, and real quaternion, respectively. Some properties of such numbers and matrices are briefly reviewed in Appendix A.

We are concerned in the present paper with the "motion" of the eigenvalues, which we denote by $x_n(\tau)\equiv E_n(\tau)$, considering the parameter τ to be a pseudotime. Differentiating both members of the eigenvalue equation,

$$\hat{H}(\tau)|n,\tau\rangle=x_n(\tau)|n,\tau\rangle \quad \text{with } \langle m,\tau|n,\tau\rangle=\delta_{mn} \ , \tag{3.2}$$

it can be shown that the parametric motion is governed by a finite set of first-order differential equations, namely,[18–21]

$$\frac{dx_n}{d\tau}=p_n \ , \tag{3.3}$$

$$\frac{dp_n}{d\tau}=2\sum_{\substack{m=1\\m\neq n}}^{N}\frac{\mathcal{L}_{nm}\mathcal{L}_{mn}}{(x_m-x_n)^3} \ , \tag{3.4}$$

$$\frac{d\mathcal{L}_{mn}}{d\tau}=-\sum_{\substack{l=1\\l\neq m,n}}^{N}\mathcal{L}_{ml}\mathcal{L}_{ln}\left[\frac{1}{(x_m-x_l)^2}-\frac{1}{(x_n-x_l)^2}\right] \ , \tag{3.5}$$

where p_n is the diagonal element of $\hat{V}$,

$$p_n(\tau)\equiv\langle n,\tau|\hat{V}|n,\tau\rangle \ , \tag{3.6}$$

and the variables $\mathcal{L}_{mn}$ are the off-diagonal elements

$$\mathcal{L}_{mn}(\tau)\equiv[x_n(\tau)-x_m(\tau)]\langle m,\tau|\hat{V}|n,\tau\rangle \ , \tag{3.7}$$

of the anti-Hermitian matrix $\hat{\mathcal{L}}$ given by

$$\hat{\mathcal{L}}\equiv[\hat{V},\hat{H}(\tau)]=[\hat{V},\hat{H}_0]=-\hat{\mathcal{L}}^{\dagger} \ , \tag{3.8}$$

which is τ independent in any τ-independent basis like in (3.1). For the symplectic systems, the elements of $\hat{\mathcal{L}}$ are real quaternion and they can be expanded on the basis of unit numbers $\{e_0,e_1,e_2,e_3\}$ as explained in Appendix A:

$$\mathcal{L}_{mn}=e_0\mathcal{L}_{mn}^{(0)}+e_1\mathcal{L}_{mn}^{(1)}+e_2\mathcal{L}_{mn}^{(2)}+e_3\mathcal{L}_{mn}^{(3)} \ . \tag{3.9}$$

Because $\hat{\mathcal{L}}$ is anti-Hermitian, $\mathcal{L}_{mn}^{(0)}$ is real antisymmetric, while the $\mathcal{L}_{mn}^{(a)}$ $(a=1,2,3)$ are real symmetric with vanishing diagonal elements. For the unitary systems, we must set $\mathcal{L}_{mn}^{(2)}$ and $\mathcal{L}_{mn}^{(3)}$ equal to zero. For the orthogonal systems, all $\mathcal{L}_{mn}^{(1)}$, $\mathcal{L}_{mn}^{(2)}$, and $\mathcal{L}_{mn}^{(3)}$ need to be set equal to zero. Keeping in mind this reduction scheme, we may consider Eq. (3.9) as providing the most complete description of the three kinds of systems.

Equations (3.3)–(3.5) are the canonical equations of the following classical Hamiltonian:[19–21]

$$\mathcal{H}_N=\tfrac{1}{2}\sum_{n=1}^{N}p_n^2+\tfrac{1}{2}\sum_{\substack{m,n=1\\m\neq n}}^{N}\sum_{a=0}^{\nu-1}\frac{(\mathcal{L}_{mn}^{(a)})^2}{(x_m-x_n)^2} \ , \tag{3.10}$$

where $\nu=1,2$, or 4 if the system is orthogonal, unitary, or symplectic, respectively. The differential equations are obtained using the Poisson brackets

$$\{x_m,p_n\}=\delta_{mn} \ , \tag{3.11}$$

and

$$\{\mathcal{L}_{kl}^{(0)},\mathcal{L}_{mn}^{(0)}\}=\tfrac{1}{2}(\delta_{km}\mathcal{L}_{ln}^{(0)}+\delta_{ln}\mathcal{L}_{km}^{(0)}-\delta_{kn}\mathcal{L}_{lm}^{(0)}-\delta_{lm}\mathcal{L}_{kn}^{(0)}) \ , \tag{3.12}$$

$$\{\mathcal{L}_{kl}^{(0)},\mathcal{L}_{mn}^{(a)}\}=\tfrac{1}{2}(\delta_{km}\mathcal{L}_{ln}^{(a)}-\delta_{ln}\mathcal{L}_{km}^{(a)}+\delta_{kn}\mathcal{L}_{lm}^{(a)}-\delta_{lm}\mathcal{L}_{kn}^{(a)}) \ , \tag{3.13}$$

$$\{\mathcal{L}_{kl}^{(a)},\mathcal{L}_{mn}^{(a)}\}=\tfrac{1}{2}(\delta_{km}\mathcal{L}_{ln}^{(0)}+\delta_{ln}\mathcal{L}_{km}^{(0)}+\delta_{kn}\mathcal{L}_{lm}^{(0)}+\delta_{lm}\mathcal{L}_{kn}^{(0)}) \ , \tag{3.14}$$

$$\{\mathcal{L}_{kl}^{(a)},\mathcal{L}_{mn}^{(b)}\}=\tfrac{1}{2}(-\delta_{km}\mathcal{L}_{ln}^{(c)}-\delta_{ln}\mathcal{L}_{km}^{(c)}-\delta_{kn}\mathcal{L}_{lm}^{(c)}-\delta_{lm}\mathcal{L}_{kn}^{(c)}) \ , \tag{3.15}$$

where *abc* represents any cyclic permutations of 123. The Poisson bracket of a pair of functions of the canonical variables is then given by

$$\{f,g\}=\sum_{n=1}^{N}\left[\frac{\partial f}{\partial x_n}\frac{\partial g}{\partial p_n}-\frac{\partial f}{\partial p_n}\frac{\partial g}{\partial x_n}\right]+\sum_{k,l,m,n=1}^{N}\sum_{a,b=0}^{\nu-1}M_{k,l,m,n}^{(a,b)}\frac{\partial f}{\partial\mathcal{L}_{kl}^{(a)}}\frac{\partial g}{\partial\mathcal{L}_{mn}^{(b)}} \ , \tag{3.16}$$

where the $M_{k,l,m,n}^{(a,b)}$ are the right-hand members of (3.12)–(3.15).

We conclude that the parametric motion of N energy levels is governed by

$$2N+\nu\frac{N(N-1)}{2} \tag{3.17}$$

canonical variables. The number (3.17) is the dimension of the phase space of the dynamical system under consideration, which is a generalized Calogero-Moser (GCM) system.[21] Strictly speaking, there exists[9,17,20] another version of the GCM system in which modified eigenstates

(rather than $\{\mathcal{L}_{mn}^{(a)}\}$) are treated as dynamical variables. While that version may be suitable for describing wave functions, the present form has the advantage of enabling us to study the statistical mechanics of energy levels. The GCM system is completely integrable because any solution $\{x_n(\tau)\}$ can be written as the zeros of the rational function

$$\det(\hat{H}_0+\tau\hat{V}-x\hat{I})=0 . \tag{3.18}$$

In order to study the statistical mechanics of the GCM system in the following sections, we introduce its Liouville measure defined by

$$\prod_{1\le m<n\le N}\prod_{a=0}^{\nu-1} dx_m\, dp_m\, d\mathcal{L}_{mn}^{(a)} . \tag{3.19}$$

IV. GENERALIZED CALOGERO-MOSER GAS

A. Grand canonical ensemble

In order to calculate the statistical properties of typical quantum systems, we need an infinite number of energy levels. This observation leads us to consider Hamiltonian operators (3.1) acting in infinite-dimensional Hilbert space. The eigenvalue spectrum can then be correlated with a gas of particles moving with the pseudotime parameter τ. The collisions between particles correspond to avoided crossings of the levels. In spite of the complete integrability of the finite GCM system, information may flow out of any finite interval in the infinite GCM system where dynamical mixing becomes possible.[22]

To study the GCM gas we need an invariant probability density defining a grand canonical ensemble. To simplify the construction, we assume that the energy spectrum extends from $-\infty$ to $+\infty$ and is invariant under x translations with a uniform density ρ. In complex quantum systems like heavy atoms, molecules, or nuclei, the level density is usually nonuniform, but for the purpose of studying the spectral fluctuations the uniform density is adequate.[14] The number of energy levels in any energy interval of size L large enough is thus assumed to follow, asymptotically, a Poisson distribution

$$W_N^L \approx \frac{(\rho L)^N}{N!} e^{-\rho L} . \tag{4.1}$$

To construct this grand canonical ensemble we introduce an intermediate canonical ensemble of systems with N particles in the interval $[-L/2,+L/2]$. At the end points $-L/2$ and $+L/2$ we place hard walls where the particles undergo elastic collisions. Between the walls the motion is ruled by the classical GCM Hamiltonian (3.10), which is used to define a Gibbs measure

$$dM_{N,L}=\frac{1}{Z_{N,L}} e^{-\beta\mathcal{H}_N} \prod_{1\le m<n\le N}\prod_{a=0}^{\nu-1} dx_m\, dp_m\, d\mathcal{L}_{mn}^{(a)} . \tag{4.2}$$

The grand canonical ensemble will then be obtained in the limit where the size L of the box increases indefinitely while keeping the density ρ constant. The resulting measure depends on two parameters: the density ρ and the inverse temperature β. The numerical value of the parameter β is determined from the variance of the velocities $\{p_n(\tau)\}$ of the energy levels:

$$\langle p_n^2\rangle-\langle p_n\rangle^2=\frac{1}{\beta},\quad \langle p_n\rangle=0 . \tag{4.3}$$

If $\langle p_n\rangle$ is different from zero in the observed spectrum, we should subtract this mean drift of the spectrum from the motion of the individual energy levels before comparing with the predictions inferred from (4.2).

To fulfill the translational invariance of the grand canonical measure, we must now verify that a uniform density of energy levels is obtained for the canonical ensemble in the limit where $L,N\to\infty$, while N/L remains constant.

B. Relationship to random matrix theory

After integrating over the variables p_m and $\mathcal{L}_{mn}^{(a)}$ we get the joint probability density of the energy levels

$$f_{N,L}(x_1,\ldots,x_n)=\frac{1}{\mathcal{N}_{N,L}}\prod_{1\le i<j\le N}|x_i-x_j|^\nu \quad \text{for } -L/2\le x_i\le +L/2 , \tag{4.4}$$

which we recognize to be the joint probability density of random matrix theory.[11,14]

The normalizing constant of (4.4), the level density, as well as the spacing distribution, are all calculated starting from the generating functional defined by

$$I_N(u)=\int_{-1}^{1}\cdots\int_{-1}^{1}\prod_{k=1}^{N}u(x_k)\prod_{1\le i<j\le N}|x_i-x_j|^\nu \times dx_1\cdots dx_N , \tag{4.5}$$

where we set the size of the box to $L=2$ for simplicity. The normalizing constant is then given by

$$\mathcal{N}_{N,L}=I_N(1)(L/2)^{N+(\nu/2)N(N-1)} , \tag{4.6}$$

where $I_N(1)$ is the integral (4.5) for the function $u(x)=1$. Accordingly, the partition function becomes

$$Z_{N,L}=I_N(1)2^{N/2}[(\pi/\beta)^{1/2}L/2]^{N+(\nu/2)N(N-1)} . \tag{4.7}$$

In random matrix theory, Mehta and Gaudin[10,11] developed methods to reduce integrals like (4.5) to the Fredholm determinant of an integral kernel composed of mutually orthogonal functions. The harmonic-oscillator eigenfunctions are used in the case of the Gaussian ensembles for which the joint probability density is (4.4) multiplied by the weight function $\exp(-\frac{1}{2}\sum_k x_k^2)$. Several other ensembles, such as the Jacobi, the Laguerre, or the Legendre ensembles, have been considered by changing the weight function in order to use the corresponding orthogonal polynomials in the reduction of the integral (4.5) by the Mehta-Gaudin techniques.[11,14,23,24] In this classification, (4.4) is the joint probability density of *the Legendre ensembles*[9,24] because the weight functions is 1 so that we need the Legendre polynomials to calculate (4.5) as shown in Appendix B. Within the Legendre ensembles (as well as within the oth-

ers), the exponent $\nu=1,2$, or 4 defines the orthogonal, the unitary, or the symplectic ensemble, respectively.

The Legendre unitary ensemble was studied by Leff and we refer the reader to his paper for this case.[24] We present in Appendix B a detailed derivation of the normalizing constant, the level density, and the spacing distribution for the Legendre orthogonal ensemble. In this way, we prove that the spacing distribution of Gaudin, Mehta, and Dyson[10-12] applies to the Legendre orthogonal ensemble, confirming the universality hypothesis.[13,25] Furthermore, this analysis enables us to construct the statistical mechanics of the GCM gas.

From Appendix B, we obtain the following results which concern the Legendre orthogonal ensemble. The normalizing constant is

$$\mathcal{N}_{N,2}=I_N(1)=2^N A_N \quad \text{with} \quad A_N=\prod_{k=0}^{N}\frac{2^k(k!)^2}{(2k)!} , \tag{4.8}$$

so that the partition function for the orthogonal systems ($\nu=1$) behaves like

$$Z_{N,L}\approx 2^{3N/2}[(\pi/\beta)^{1/2}L/4]^{(1/2)N(N+1)} \quad \text{for } N\to\infty . \tag{4.9}$$

The level density is approximately given near $x=0$ by

$$\sigma_{N,L}(x)\approx\frac{2N}{\pi L}[1-(2x/L)^2]^{-1/2} \quad \text{for } N\to\infty , \tag{4.10}$$

while it rises to

$$\sigma_{N,L}(\pm L/2)=\frac{N(N+1)}{2L} , \tag{4.11}$$

near the walls of the box where the levels accumulate because of the Wigner repulsion. Inside the box and far from the walls the level density (4.10) is linear in N, in contrast to the level density for the Gaussian ensembles which has the disadvantage of increasing like $N^{1/2}$. Consequently, we define the density by

$$\rho\equiv\frac{2N}{\pi L} , \tag{4.12}$$

when we take the thermodynamic limit, $N,L\to\infty$ with $N/L=$const, to reach the grand canonical measure.

V. SPACING DISTRIBUTION

Given the large amount of interest focused on the spacing distribution it is important to derive it carefully in the present formalism. Working with the dimensionless spacing between two nearest-neighbor levels $x_n<x_{n+1}$,[11]

$$S=(\text{spacing/mean spacing})=\rho(x_{n+1}-x_n) , \tag{5.1}$$

the spacing density $p(S)$ is the second derivative of the probability $\mathcal{E}(S)$ that an interval of size S is empty of eigenvalues[11]

$$p(S)=\frac{d^2\mathcal{E}(S)}{dS^2} . \tag{5.2}$$

We prove in Appendix B 4 that $\mathcal{E}(S)$ is identical, for the Legendre orthogonal ensemble, to the universal function obtained by Gaudin, Mehta, and Dyson for the Gaussian and circular orthogonal ensembles, namely,[10,11,26]

$$p_{\mathrm{OE}}(S)=\frac{\pi^2}{6}S-\frac{\pi^4}{60}S^3+\frac{\pi^4}{270}S^4+\frac{\pi^6}{1680}S^5+\cdots . \tag{5.3}$$

This result completes the proof by Leff[24] that the spacing distribution for the Legendre unitary ensemble is the corresponding universal one[11,25]

$$p_{\mathrm{UE}}(S)=\frac{\pi^2}{3}S^2-\frac{2\pi^4}{45}S^4+\frac{\pi^6}{315}S^6+\cdots , \tag{5.4}$$

with now a quadratic repulsion. Assuming the universality of the different ensembles,[13,25] we conjecture that the spacing density for the Legendre symplectic ensemble will be the Mehta-Dyson form[26]

$$p_{\mathrm{SE}}(S)=\frac{2^4\pi^4}{135}S^4-\frac{2^7\pi^6}{4725}S^6+\cdots , \tag{5.5}$$

with a quartic repulsion. We shall need these results in Sec. VI.

VI. TAIL OF THE CURVATURE DISTRIBUTION

From the definition (1.2) of the curvature, we observe that the curvature of the level $x_1(\tau)$ is identical to its acceleration given by (3.4), so that

$$K\equiv\ddot{x}_1(\tau)=-\frac{\partial\mathcal{H}_N}{\partial x_1} . \tag{6.1}$$

The probability density for the curvature of x_1 to take the value K is then defined by[9]

$$\mathcal{P}(K)\equiv\lim_{\substack{N/L\to\infty\\ N/L=\text{const}}}\mathcal{P}_{N,L}(K) , \tag{6.2}$$

with

$$\mathcal{P}_{N,L}(K)\equiv\int\delta\left[K+\frac{\partial\mathcal{H}_N}{\partial x_1}\right]dM_{N,L} , \tag{6.3}$$

where $dM_{N,L}$ is the Gibbs measure (4.2).

In the following, we shall calculate the asymptotic expansion of the probability density (6.2) when K is large. By this approach, we evaluate the probability for rare large curvatures to occur in the parametric motion of the energy levels in irregular spectra. From Eq. (3.4), the equation

$$K+\frac{\partial\mathcal{H}_N}{\partial x_1}=0 , \tag{6.4}$$

possesses $N-1$ roots $\{x_1^{(k)}\}$ for any value of K. These zeros can be evaluated when K is large, positive, or negative, because (6.1) is a function of x_1 which diverges in the vicinity of each level different from x_1. Choosing K positive we obtain

$$x_1^{(k)}\approx x_k+\left[\frac{2}{K}\sum_a(\mathcal{L}_{1k}^{(a)})^2\right]^{1/3} . \tag{6.5}$$

Consequently, we get

$$\mathcal{P}_{N,L}(K)=\sum_{k=2}^{N}\int\left|\frac{\partial^2\mathcal{H}_N}{\partial x_1^2}\right|^{-1}\delta(x_1-x_1^{(k)}(K))dM_{N,L} , \tag{6.6}$$

with

$$\frac{\partial^2 \mathcal{H}_N}{\partial x_1^2}(x_1^{(k)}) \approx 3\left[\frac{2}{K^4}\sum_a (\mathcal{L}_{1k}^{(a)})^2\right]^{-1/3} . \tag{6.7}$$

Introducing the expression (4.2) for the measure and carrying out a straightforward integration, the details of which are given in Appendix C, we obtain

$$\mathcal{P}_{N,L}(K) \approx \frac{\mathcal{M}_{N,L}}{\mathcal{N}_{N,L}} \frac{2^{2\nu-3}(\nu+2)!}{\beta^{\nu+1}K^{\nu+2}} , \tag{6.8}$$

where $\mathcal{N}_{N,L}$ is the normalizing constant (4.6) and $\mathcal{M}_{N,L}$ is the integral (C6) given in the Appendix C. The ratio of these latter quantities can be rewritten as the following mean value over the joint probability density (4.4):

$$\frac{\mathcal{M}_{N,L}}{\mathcal{N}_{N,L}} = \left\langle \sum_{k(\neq 1)} \frac{\delta(x_1 - x_k)}{|x_1 - x_k|^\nu} \right\rangle . \tag{6.9}$$

In the thermodynamic limit, and far from the hard walls, this expression is related to the spacing density at zero spacing by

$$\lim_{\substack{N,L\to\infty \\ N/L=\text{const}}} \frac{\mathcal{M}_{N,L}}{\mathcal{N}_{N,L}} = \rho^{\nu+1} \lim_{S\to 0} S^{-\nu} p(S) \equiv D_\nu \rho^{\nu+1} , \tag{6.10}$$

where ρ is the level density and the constants D_ν are determined from Eqs. (5.3)–(5.5) (cf. Appendix C 2 and cf. Ref. 27 for the case $\nu=1$). The result is similar for negative K.

Finally, the tail of the curvature distribution is given for each ensemble by

$$\mathcal{P}_{\text{OE}}(K) = \frac{\pi^2}{2}\left[\frac{\rho}{\beta}\right]^2 \frac{1}{|K|^3} + \cdots , \tag{6.11}$$

$$\mathcal{P}_{\text{UE}}(K) = 2^4\pi^2\left[\frac{\rho}{\beta}\right]^3 \frac{1}{K^4} + \cdots , \tag{6.12}$$

$$\mathcal{P}_{\text{SE}}(K) = \frac{2^{13}\pi^4}{3}\left[\frac{\rho}{\beta}\right]^5 \frac{1}{K^6} + \cdots , \tag{6.13}$$

for large $|K|$. We note that the powers of the parameters β and ρ are consistent with the fact that the dimensionless curvature is

$$\beta K/\rho . \tag{6.14}$$

This result provides the justification for the scaling (2.4) needed when the spectrum is nonuniform.

The curvature distributions (6.11)–(6.13) are normalizable so that they have a probabilistic interpretation. Their mean value is zero because the densities are symmetric under $K \to -K$. The variance is infinite for the orthogonal ensemble but finite for the unitary and the symplectic ensembles.

Because the level curvature is the acceleration of a particle in the GCM gas, the curvature distribution is the analog of the Holtsmark distribution for a gas of stars interacting by gravitation.[28] However, the present distributions are not stable in the sense of Lévy, as is the case for the Holtsmark distribution. Whether they are infinitely divisible distributions is an open question.

VII. NUMERICAL RESULTS

In order to check the asymptotic expressions (6.11)–(6.13) for the curvature densities, we need good statistics for the energy levels. Accordingly, we carried out a numerical simulation with an ensemble of parametric systems (3.1) with random real, complex, and real quaternion Hermitian matrices $\hat{H}_0$ and $\hat{V}$ taken in Gaussian ensembles of density[11,14]

$$C_0 e^{-a_0 \text{Tr}\hat{H}_0^2} \prod_{1\le k\le N} dH_{0kk}^{(0)} \prod_{1\le k<l\le N} \prod_{a=0}^{\nu-1} dH_{0kl}^{(a)} , \tag{7.1}$$

and

$$C_1 e^{-a_1 \text{Tr}\hat{V}^2} \prod_{1\le k\le N} dV_{kk}^{(0)} \prod_{1\le k<l\le N} \prod_{a=0}^{\nu-1} dV_{kl}^{(a)} , \tag{7.2}$$

where we fixed $a_0 = \frac{1}{4}$ and $a_1 = \frac{1}{16}$. C_0 and C_1 are the normalizing constants. The spectra of these systems are already irregular at $\tau=0$. A suitable shift of the origin of τ always guarantees this situation. We can calculate the curvature of each level thanks to the second-order perturbation formula

$$\ddot{x}_n = 2\sum_{\substack{m=1 \\ m\neq n}}^{N} \sum_{a=0}^{\nu-1} \frac{(V_{mn}^{(a)})^2}{x_n - x_m} , \tag{7.3}$$

where the $\{x_n\}$ are the eigenvalues of the matrix $\hat{H}_0$. Because the probability density (7.2) is invariant under any orthogonal, unitary, or symplectic transformation $\hat{V} \to \hat{W}^{-1}\hat{V}\hat{W}$, the matrix elements $V_{mn}^{(a)}$ of $\hat{V}$ in the basis

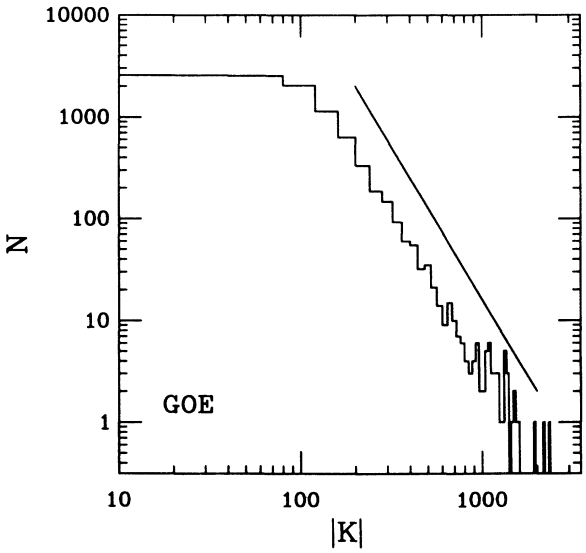

FIG. 6. Density of the level curvature (in absolute value) obtained from 50 pairs $(\hat{H}_0, \hat{V})$ of random (200×200) real symmetric matrices taken in the Gaussian orthogonal ensemble (GOE) described in Sec. VII. The histogram of the absolute value of the level curvature is constructed with cells of size $\Delta|K| = 40$. The histogram is plotted in logarithmic scale. The solid line has a slope −3.

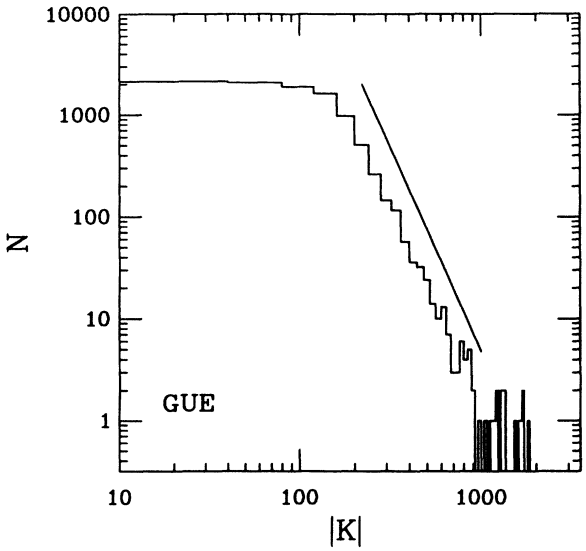

FIG. 7. Density of the level curvature (in absolute value) obtained from 50 pairs of random (200×200) complex Hermitian matrices taken in the Gaussian unitary ensemble (GUE). The solid line has a slope −4.

of eigenstates of $\hat{H}_0$ have the same Gaussian density (7.2).[11]

The histograms of the absolute values of the curvature were then calculated for the orthogonal, unitary, and symplectic ensembles, and plotted in Figs. 6, 7, and 8, respectively. Each figure also shows the theoretical slope expected from Eqs. (6.11)–(6.13) for $\log\mathcal{P}(K)$ versus $\log|K|$. The agreement is excellent.

We note that the Gaussian ensembles used for this numerical calculation are not the Legendre ensembles used in the theoretical calculation. The agreement suggests

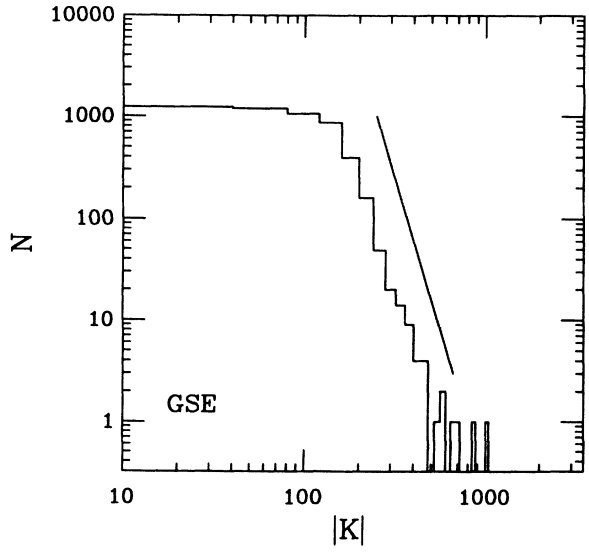

FIG. 8. Density of the level curvature (in absolute value) obtained from 50 pairs of random (100×100) real-quaternion Hermitian matrices taken in the Gaussian symplectic ensemble (GSE) (see Sec. VII). The solid line has a slope −6.

that the curvature distribution is independent of the details of the ensembles when the conditions defining the Dyson universality classes[13] are met.

VIII. CONCLUSIONS

In this paper we have obtained the tails of the curvature densities [given by Eqs. (6.11)–(6.13)] for the orthogonal, unitary, and symplectic ensembles. The detailed calculation we give here confirms the elementary derivation of the tail function based on the assumption that the curvature of a level is determined by its nearest neighbors. Indeed, the second-order perturbation formula (7.3) suggests that $K\sim S^{-1}$. If the spacing density behaves like S^{ν} near $S=0$, the curvature density then decreases like $|K|^{-\nu-2}$ for large $|K|$, as obtained previously.[9] This close relationship between both distributions leads us to conjecture that the distributions of the dimensionless curvature (2.4) or (6.14) are universal, as the spacing distributions within the three universality classes of Dyson.[13,25]

Although the present theory concerns autonomous quantum systems (3.1), the extension of the results of Secs. III–VI to periodically kicked quantum systems like (2.5) is possible. The statistical mechanics of quasienergy levels for periodically driven systems has recently been investigated in Ref. 29. Nakamura and Mikeska showed that the parametric motion of the quasienergy eigenvalues is governed by the Sutherland system of differential equations.[17] Gibbs ensembles based on this classical Hamiltonian reduce to the Dyson circular ensembles of random matrix theory.[13,14] The grand canonical ensemble of the infinite GCM systems defined in Sec. IV is recovered in the limit where the number of quasienergy eigenvalues becomes infinite on the unit circle, so that we expect that the curvature distributions (6.11)–(6.13) also hold for periodically kicked systems with many level irregular spectra.

We believe that these curvature distributions can be experimentally observed in the spectra of atomic or molecular systems in an external electric or magnetic field.[1,2,6] The curvature distribution can be constructed from energy spectra taken with at least three close values of the external field. The determination of the tail exponent requires, typically, several hundred level curvatures. The statistics can be improved by measuring the curvature of the same levels but at several different values of the external field, values which are sufficiently separated from each other. Moreover, the use of the distribution function $\mathcal{I}(|K|)$ rather than the density is recommended because we thus avoid the problem of choosing a good cell size for the histogram. From Eqs. (6.11)–(6.13), we deduce that

$$\lim_{|K|\to\infty}\frac{\log[1-\mathcal{I}(|K|)]}{\log|K|^{-1}}=\nu+1\ . \tag{8.1}$$

The measurement of such statistical quantities introduces a new way of describing irregular spectra. If the level spacings or the spectral rigidity were determined by the spectrum with the perturbation parameter τ fixed once and for all, the curvature would provide a characterization of the sensitivity of the irregular energy spec-

trum to variation of a perturbation parameter. In particular, the theory developed in the present paper completes the Brownian motion model approach proposed by Dyson.[27,30–32] Interpreting the perturbation parameter τ as a pseudotime, a Newtonian theory of ensembles based on the GCM Hamiltonian (3.10) can now be constructed, thereby filling a missing link in the program started by Dyson. Indeed, if stochastic Brownian motion describes the trajectories $x_n(\tau)$ of the GCM gas on a large scale, the here-defined curvature (or acceleration) distribution describes the small-scale differentiable structure of the energy-level trajectories.

On the other hand, new ensembles can now be invented and numerically implemented. In particular, the Legendre ensembles can be simulated by the numerical integration of the GCM differential equations for N particles in a box of size L with hard walls. We also remark that the parametric distortions of an irregular spectrum are characterized here by a temperature β^{-1} which is naturally interpreted as the variance of the velocity of the energy levels when the parameter τ varies [see Eqs. (4.3)]. Accordingly, the present Newtonian ensembles distinguish the temperature β from the exponents ν labeling the universality classes of Dyson, albeit both are identical in the Coulomb gas model.

Furthermore, the introduction of the pseudotime τ in addition to the pseudoposition x introduces a new ergodic property of infinite GCM systems, defined by the equality of an ensemble average and a pseudotime average. This ergodic property is different from the ergodicity defined when an ensemble average equals a pseudoposition average, which has been previously considered in random matrix theory.[5] The new pseudotime ergodicity is known to exist for the ideal gas and the harmonic solid, both of which share several features with the GCM gas.

Finally, the level curvature plays an important role in the magnetic susceptibility. In a random medium or in size-effect quantum systems, the statistical properties of the parametric motion of the energy levels are required for the prediction of magnetic properties.[33]

ACKNOWLEDGMENTS

P.G. is grateful to Professor G. Nicolis for his support. P.G. would like to thank the National Funds for Scientific Research (Belgium) for financial support.

APPENDIX A: QUATERNIONS

Real quaternions are real linear combinations of the unit numbers $\{e_0,e_1,e_2,e_3\}$ which satisfy the multiplication rules[11,14]

$$e_0^2=e_0,\quad e_a^2=-e_0\ , \tag{A1}$$

and

$$e_0e_a=e_ae_0=e_a,\quad e_ae_b=-e_be_a=e_c\ , \tag{A2}$$

where abc is a cyclic permutation of 123. These unit numbers can be represented by 2×2 matrices with complex elements.[11,14] The Hermitian conjugates of these unit members are defined by

$$e_0^+=e_0,\quad e_a^+=-e_a\quad (a=1,2,3)\ . \tag{A3}$$

If $\hat{A}$ is a matrix with real quaternions elements, its Hermitian conjugate has the elements

$$(\hat{A}^\dagger)_{mn}=(\hat{A})^+_{nm}\ . \tag{A4}$$

The complex numbers form a subset of the real quaternion numbers where the components of e_2 and e_3 are zero. We may then use the standard notation with the identification $e_0\equiv1$ and $e_1\equiv(-1)^{1/2}$, whereupon the Hermitian conjugacy reduces to complex conjugacy. The real numbers form a subset of the real quaternions where the components of e_1, e_2, and e_3 are zero.

APPENDIX B: LEGENDRE ORTHOGONAL ENSEMBLE

The following calculations follow closely Chap. 5 of the book by Mehta.[11] However, the extrapolation to the Legendre orthogonal ensemble is not straightforward. The main difficulty is the nonvanishing of the Legendre polynomials at the boundaries of the interval $[-1,1]$, albeit the harmonic oscillator eigenfunctions used for the Gaussian ensembles vanish at the boundaries of their domain of definition, namely $(-\infty,\infty)$. In order to overcome this problem, further manipulations are needed.

In this appendix, we set $L=2$ so that the energy levels are confined in the interval $[-1,1]$. To treat the Legendre orthogonal ensemble, we choose the exponent $\nu=1$ in the generating functional $I_N(u)$ given by Eq. (4.5). Furthermore, we restrict ourselves to even values of the number N of energy levels to simplify the calculations.

1. The generating functional

We summarize the different steps required to integrate (4.5).

(a) The domain $[-1,1]^N$ is decomposed into te $N!$ subdomains where the variables $\{x_i\}$ are ordered. Because the integrand of (4.5) is a symmetric function, $I_N(u)$ is equal to $N!$ times the integral of the same integrand but over anyone of these subdomains. For definiteness we choose

$$R=\{-1<x_1<x_2<\cdots<x_N<1\}. \tag{B1}$$

Because the variables are now ordered, the product $\prod_{i<j}|x_i-x_j|$ is equal to the Vandermonde determinant

$$\det[(x_i)^{j-1}]_{i,j=1,\ldots,N}\ . \tag{B2}$$

(b) Using the property of the Legendre polynomials that

$$P_n(x)=\frac{(2n)!}{2^n(n!)^2}x^n+O(x^{n-1})\ , \tag{B3}$$

the integral (4.5) becomes

$$I_N(u)=N!A_{N-1}\int\cdots\int_R\det[u(x_i)P_{j-1}(x_i)]_{i,j=1,\cdots,N}\times dx_1\cdots dx_N\ , \tag{B4}$$

with

$$A_{N-1}=\prod_{k=0}^{N-1}\frac{2^k(k!)^2}{(2k)!}\ . \tag{B5}$$

(c) (B4) can then be expressed as a Pfaffian (cf. Refs. 10 and 11)

$$I_N(u)=N!\,A_{N-1}[\det(f_{kl})_{k,l=0,\ldots,N-1}]^{1/2}\ , \tag{B6}$$

with

$$f_{kl}=\int_{-1}^{1}dx\int_{-1}^{x}dy\,u(x)u(y)[P_k(x)P_l(y)-P_k(y)P_l(x)]\ . \tag{B7}$$

The indices k and l are separated into even and odd numbers by permutations of lines and columns in $\det(f_{kl})$ so that the indices are ordered like

$$k,l=0,2,4,\ldots,N-2;\quad N-1,1,3,\ldots,N-3\ . \tag{B8}$$

Note that the odd integer $N-1$ is placed in front of the other odds in order to deal with the nonvanishing of the Legendre polynomials at ±1, as will appear below.

(d) Using the property of the Legendre polynomials that

$$P'_{2j}(x)=(4j-1)P_{2j-1}(x)+(4j-5)P_{2j-3}(x)+\cdots+3P_1(x)\ , \tag{B9}$$

and forming linear combinations of lines and columns, $\det(f_{kl})$ is transformed into $\det(\tilde f_{kl})$ with the elements

$$\tilde f_{2i,2j}=\int_{-1}^{1}dx\int_{-1}^{x}dy\,u(x)u(y)[P_{2i}(x)P_{2j}(y)-P_{2i}(y)P_{2j}(x)]\ , \tag{B10}$$

$$\tilde f_{2i,2j-1}=\frac{1}{4j-1}\int_{-1}^{1}dx\int_{-1}^{x}dy\,u(x)u(y)\times[P_{2i}(x)P'_{2j}(y)-P_{2i}(y)P'_{2j}(x)]\ , \tag{B11}$$

$$\tilde f_{2i-1,2j-1}=\frac{1}{(4i-1)(4j-1)}\times\int_{-1}^{1}dx\int_{-1}^{x}dy\,u(x)u(y)[P'_{2i}(x)P'_{2j}(y)-P'_{2i}(y)P'_{2j}(x)]\ . \tag{B12}$$

(e) The columns $\tilde f_{kl}$ with $l=1,3,\ldots,N-3$ are replaced by

$$(2l+1)(2l+3)\left[\tilde f_{kl}-\frac{2N-1}{2l+1}\tilde f_{k,N-1}\right]\ . \tag{B13}$$

The column $\tilde f_{k,N-1}$ is replaced by $-\tilde f_{k,N-1}$. Similar transformations are carried out on the lines $k=N-1,1,3,\ldots,N-3$. All the lines are then divided by 4. Accordingly,

$$\det(\tilde f_{kl})=\left[\frac{2^N}{3\times5\times7\times\cdots\times(2N-3)(2N-1)}\right]^2\times\det\begin{bmatrix}\lambda_{ij}&g_{ij}\\-g_{ji}&\mu_{ij}\end{bmatrix}\ , \tag{B14}$$

where

$$\lambda_{ij}=\tfrac14\int_{-1}^{1}dx\int_{-1}^{x}dy\,u(x)u(y)[P_{2i}(x)P_{2j}(y)-P_{2i}(y)P_{2j}(x)]=-\lambda_{ji}\ , \tag{B15}$$

$$g_{ij}=\frac{4j+1}{4}\int_{-1}^{1}dx\int_{-1}^{x}dy\,u(x)u(y)[P_{2i}(x)\phi_{2j}(y)-P_{2i}(y)\phi_{2j}(x)]\ , \tag{B16}$$

$$\mu_{ij}=\frac{(4i+1)(4j+1)}{4}\int_{-1}^{1}dx\int_{-1}^{x}dy\,u(x)u(y)[\phi_{2i}(x)\phi_{2j}(y)-\phi_{2i}(y)\phi_{2j}(x)]=-\mu_{ji}\ , \tag{B17}$$

with

$$\phi_{2i}(x)=P'_{2i}(x)-P'_N(x),\quad i,j=0,1,2,\ldots,N/2-1\ . \tag{B18}$$

We remark that the line and the column labeled by k or $l=N-1$ in $\tilde f_{kl}$ are transformed into the column $j=0$ of g_{ij} and μ_{ij} as well as the line $i=0$ of μ_{ij}. They are not further separated from the other columns and lines in the notation of Eqs. (B16) and (B17). In this way, we are able to calculate exactly the generating functional of the Legendre orthogonal ensemble.

(f) Finally, the integral (4.5) becomes

$$I_N(u)=2^N A_N\left[\det\begin{bmatrix}\lambda_{ij}&g_{ij}\\-g_{ji}&\mu_{ij}\end{bmatrix}\right]^{1/2}\ . \tag{B19}$$

2. Normalizing constant

This constant is obtained by using the function $u(x)=1$ in (B15)–(B17). We obtain

$$\lambda_{ij}=\mu_{ij}=0,\quad g_{ij}=\delta_{ij}\ , \tag{B20}$$

which justifies by its simplicity the previous manipulations. Accordingly, the normalizing constant is given by Eq. (4.8).

3. Level density

Dyson showed that the level density as well as the n-level correlation functions are obtained from the functional derivatives with respect to the function $a(x)$ of the functional (B19), where the function $u(x)$ is replaced by $1+a(x)$.[12] In particular, the level density is given by[11]

$$\sigma_{N,2}(x)\equiv\left[\frac{\delta}{\delta a(x)}\frac{I_N(1+a)}{I_N(1)}\right]_{a=0}$$
$$=\left[\frac{\delta}{\delta a(x)}\sum_{i=0}^{N/2-1}\nu_{ii}\right]_{a=0}, \quad \text{(B21)}$$

where

$$\nu_{ij}\equiv g_{ij}-\delta_{ij} . \quad \text{(B22)}$$

Using the expansion (B9) of the even Legendre polynomial derivatives, together with the odd polynomial corresponding formula, we obtain

$$\sigma_{N,2}(x)=\sum_{k=0}^{N-1}\frac{2k+1}{2}[P_k(x)]^2-\tfrac{1}{2}P_N(x)P'_{N-1}(x) . \quad \text{(B23)}$$

Using the Christoffel-Darboux formula and the derivative recurrence formula,[34] we finally have

$$\sigma_{N,2}(x)=\frac{N}{2(1-x^2)}[NP^2_{N-1}(x)+(N+1)P^2_N(x)-(2N+1)xP_{N-1}(x)P_N(x)] . \quad \text{(B24)}$$

Using large-order expansion of the Legendre polynomials, Eq. (4.10) is obtained after the rescaling $x\to 2x/L$. Equation (4.11) is derived starting from (B23) with the analog of Eq. (B9) for odd Legendre polynomials and $P_n(\pm 1)=(\pm 1)^n$.

4. Spacing distribution

The spacing density is the second derivative of the probability $\mathcal{E}_N(\theta)$ that the interval $[-\theta,+\theta]$ with $\theta<1$ is empty of levels.[11] This probability is given by

$$\mathcal{E}_N(\theta)=I_N(u)/I_N(1) , \quad \text{(B25)}$$

with

$$u(x)=\begin{cases}0, & -\theta<x<+\theta,\\ 1, & \theta<|x|.\end{cases} \quad \text{(B26)}$$

Because (B26) is an even function of x,

$$\lambda_{ij}=\mu_{ij}=0 , \quad \text{(B27)}$$

and

$$\mathcal{E}_N(\theta)=\det(g_{ij})_{i,j=0,\cdots,N/2-1} . \quad \text{(B28)}$$

After integration, we get

$$g_{ij}=\delta_{ij}-M_{ij} , \quad \text{(B29)}$$

with

$$M_{ij}(\theta)=\frac{4j+1}{2}\int_{-\theta}^{\theta}P_{2i}(x)[P_{2j}(x)-P_N(x)]dx . \quad \text{(B30)}$$

Given this expression, we apply the method of Mehta and Gaudin to calculate $\mathcal{E}_N(\theta)$.[10,11] We have the identity

$$\det[\hat{I}-\hat{M}(\theta)]=\prod_{k=0}^{N/2-1}(1-\lambda_k) , \quad \text{(B31)}$$

provided that $\{\lambda_k\}$ are the eigenvalues of the matrix (B30). They are also the eigenvalues

$$\lambda f(x)=\int_{-\theta}^{\theta}\mathcal{K}_N(x,y)f(y)dy \quad \text{(B32)}$$

of the kernel

$$\mathcal{K}_N(x,y)=\sum_{i=0}^{N/2-1}\frac{4i+1}{2}P_{2i}(x)[P_{2i}(y)-P_N(y)] , \quad \text{(B33)}$$

acting on the functions

$$f(x)=\sum_{i=0}^{N/2-1}c_iP_{2i}(x) . \quad \text{(B34)}$$

We note that the kernel (B33) characterizes the Legendre orthogonal ensemble and differs from the kernels calculated previously for the other ensembles.

In the limit $N\to\infty$, using the Christoffel-Darboux formula together with the large-order asymptotic expansion of the Legendre polynomials,[34]

$$P_{2m}\left[\frac{\pi\xi}{2m}\right]\approx\frac{(-1)^m}{(\pi m)^{1/2}}\cos(\pi\xi) , \quad \text{(B35)}$$

and

$$P_{2m+1}\left[\frac{\pi\xi}{2m}\right]\approx\frac{(-1)^m}{(\pi m)^{1/2}}\sin(\pi\xi) , \quad \text{(B36)}$$

the kernel becomes

$$\lim_{N\to\infty}\frac{\pi}{N}\mathcal{K}_N\left[\frac{\pi\xi}{N},\frac{\pi\eta}{N}\right]=\frac{1}{2}\left[\frac{\sin[\pi(\xi-\eta)]}{\pi(\xi-\eta)}+\frac{\sin[\pi(\xi+\eta)]}{\pi(\xi+\eta)}\right] , \quad \text{(B37)}$$

which is the universal kernel obtained by Gaudin and Mehta.[10,11] Accordingly,

$$\mathcal{E}(S)\equiv\lim_{N\to\infty}\mathcal{E}_N(\pi S/2N)=\prod_{i=0}^{\infty}[1-S\gamma^2_{2i}(S)] , \quad \text{(B38)}$$

where

$$\gamma_{2i}(S)=\frac{1}{2f_{2i}(0;S)}\int_{-1}^{1}f_{2i}(z;S)dz , \quad \text{(B39)}$$

in terms of the S-dependent spheroidal functions $f_0,f_2,f_4,\ldots$, as proved by Gaudin and Mehta.[10,11]

APPENDIX C: TAIL OF THE CURVATURE DENSITY

1. Asymptotic expansion

Equation (6.6) is evaluated asymptotically for large and positive values of K. After integration over the variables x_1, $\{p_n\}$, and $\{\mathcal{L}^{(a)}_{mn}\}$, with m and n different from 1 , we obtain

$$\mathcal{P}_{N,L}(K)=\frac{1}{Z_{N,L}}\left[\frac{2\pi}{\beta}\right]^{N/2}\sum_{k=2}^{N}\int\left|\frac{\partial^2\mathcal{H}_N}{\partial x_1^2}(x_1^{(k)})\right|^{-1}\exp\left[-\beta\sum_{n=2}^{N}\sum_{a}\frac{(\mathcal{L}_{1n}^{(a)})^2}{(x_1^{(k)}-x_n)^2}\right]$$
$$\times\prod_{2\le i<j\le N}[(\pi/\beta)^{1/2}|x_i-x_j|]^{\nu}dx_2\cdots dx_N\prod_{a}d\mathcal{L}_{12}^{(a)}\cdots\mathcal{L}_{1N}^{(a)}\ . \tag{C1}$$

From the asymptotic expression (6.5) for the root $x_1^{(k)}$, we have

$$\sum_{n=2}^{N}\sum_{a}\frac{(\mathcal{L}_{1n}^{(a)2})}{(x_1^{(k)}-x_n)^2}=\left[\frac{K^2}{4}\sum_{a}(\mathcal{L}_{1k}^{(a)})^2\right]^{1/3}+\sum_{\substack{n=2\\n\neq k}}^{N}\sum_{a}\frac{(\mathcal{L}_{1n}^{(a)})^2}{(x_k-x_n)^2}+O(K^{-1/3})\ . \tag{C2}$$

Replacing the second derivative of the GCM Hamiltonian by (6.7) and integrating over the variable $\{\mathcal{L}_{1n}^{(a)}\}$, with $n\neq k$ in the kth term, (C1) becomes

$$\mathcal{P}_{N,L}(K)\approx\frac{1}{Z_{N,L}}\left[\frac{2\pi}{\beta}\right]^{N/2}\sum_{k=2}^{N}\mathcal{T}_{\nu}^{(k)}\int_{[-L/2,L/2]^{N-1}}\prod_{2\le i<j\le N}[(\pi/\beta)^{1/2}|x_i-x_j|]^{\nu}\prod_{\substack{n=2\\n\neq k}}^{N}[(\pi/\beta)^{1/2}|x_k-x_n|]^{\nu}dx_2\cdots dx_N\ , \tag{C3}$$

where

$$\mathcal{T}_{\nu}^{(k)}=\int_{(-\infty,+\infty)^{\nu}}\frac{1}{3}\left[\frac{2}{K^4}\sum_{a}(\mathcal{L}_{1k}^{(a)})^2\right]^{1/3}\exp\left[-\beta\left[\frac{K^2}{4}\sum_{a}(\mathcal{L}_{1k}^{(a)})^2\right]^{1/3}\right]\prod_{a=0}^{\nu-1}d\mathcal{L}_{1k}^{(a)}\ , \tag{C4}$$

with $0\le a\le\nu-1$. This integral is independent of the index k and is given by

$$\mathcal{T}_{\nu}^{(k)}=\frac{\pi^{\nu/2}2^{2\nu-3}(\nu+2)!}{\beta^{3\nu/2+1}K^{\nu+2}}\ . \tag{C5}$$

Finally, introducing

$$\mathcal{M}_{N,L}\equiv\sum_{k=2}^{N}\int_{-L/2}^{+L/2}\cdots\int_{-L/2}^{+L/2}\prod_{2\le i<j\le N}|x_i-x_j|^{\nu}\prod_{\substack{n=2\\n\neq k}}^{N}|x_k-x_n|^{\nu}dx_2\cdots dx_N\ , \tag{C6}$$

and using Eqs. (4.6) and (4.7), we obtain Eq. (6.8).

2. The coefficient

We evaluate here the mean value (6.9) for a uniform spectrum of density ρ. Let x_0 be any eigenvalue in a sequence,

$$\cdots<x_{-2}<x_{-1}<x_0<x_1<x_2<\cdots\ , \tag{C7}$$

of ordered eigenvalues. The distribution $\delta(x)$ in (6.9) is replaced by the function

$$\Delta_{\epsilon}(x)=\begin{cases}0 & \text{for } |x|>\epsilon/2,\\ 1/\epsilon & \text{for } |x|<\epsilon/2.\end{cases} \tag{C8}$$

Then Eq. (6.9) becomes a series of terms each containing a pair of mean values:

$$\sum_{m=0}^{\infty}\left\{\left\langle\frac{\Delta_{\epsilon}(x_0-x_{m+1})}{|x_0-x_{m+1}|^{\nu}}\right\rangle+\left\langle\frac{\Delta_{\epsilon}(x_0-x_{-m-1})}{|x_0-x_{-m-1}|^{\nu}}\right\rangle\right\}\ . \tag{C9}$$

The mth term is given by

$$\rho^{\nu+1}\frac{2}{\epsilon}\int_0^{\epsilon/2}S^{-\nu}p^{(m)}(S)dS\quad(m=0,1,2,\ldots)\ , \tag{C10}$$

where $p^{(m)}(S)$ is the density of the mth-order spacing distribution.[14,35] For $m=0$, $p^{(0)}(S)$ is the nearest-neighbor spacing density given by (5.3)–(5.5) for $\nu=1,2$, and 4, respectively. In the limit $\epsilon\to0$ and when $m=0$, (C10) gives (6.10). However, the densities of the higher-order spacing distributions are known to vanish at $S=0$ with powers greater than ν.[14,35] Accordingly, (C10) with $m\ge1$ vanishes and (C9) reduces to (6.10). Q.E.D.

[1]M. G. Littman, M. L. Zimmerman, T. W. Ducas, R. R. Freeman, and D. Kleppner, Phys. Rev. Lett. **36**, 788 (1976); M. G. Littman, M. L. Zimmerman, and D. Kleppner, *ibid.* **37**, 486 (1976); M. L. Zimmerman, M. G. Littman, M. M. Kash, and D. Kleppner, Phys. Rev. A **20**, 2251 (1979); J. R. Rubbmark, M. M. Kash, M. G. Littman, and D. Kleppner, *ibid.* **23**, 3107 (1981).

[2]M. L. Zimmerman, J. C. Castro, and D. Kleppner, Phys. Rev. Lett. **40**, 1083 (1978); C. Iu, G. R. Welch, M. M. Kash, L. Hsu, and D. Kleppner, *ibid.* **63**, 1133 (1989).

[3]I. C. Percival, J. Phys. B **6**, L229 (1973).

[4]O. Bohigas, M. J. Giannoni, and C. Schmidt, Phys. Rev. Lett.

52, 1 (1984); D. Delande and J. C. Gay, *ibid*, **57**, 2006 (1986); D. Wintgen and H. Marxer, *ibid*. **60**, 971 (1988).

[5]T. A. Brody, J. Flores, J. B. French, P. A. Mello, A. Pandey, and S. S. M. Wong, Rev. Mod. Phys. **53**, 385 (1981).

[6]H. S. Camarda and P. D. Georgopoulos, Phys. Rev. Lett. **50**, 492 (1983); E. Haller, H. Köppel, and L. S. Cederbaum, Chem. Phys. Lett. **101**, 215 (1983); Th. Zimmermann, H. Köppel, L. S. Cederbaum, G. Persch, and W. Demtröder, Phys. Rev. Lett. **61**, 3 (1988).

[7]N. Pomphrey, J. Phys. B **7**, 1909 (1974); D. W. Noid, M. L. Koszykowski, M. Tabor, and R. A. Marcus, J. Chem. Phys. **72**, 6169 (1980); J. Brickmann and R. D. Levine, Chem. Phys. Lett. **120**, 252 (1985).

[8]M. Wilkinson, J. Phys. A **22**, 2795 (1989); J. Goldberg, U. Smilansky, M. V. Berry, W. Schweizer, G. Wunner, and G. Zeller (unpublished).

[9]P. Gaspard, S. A. Rice, and K. Nakamura, Phys. Rev. Lett. **63**, 930 (1989); a misprint appears in Eq. (14) of this paper, which was corrected in Phys. Rev. Lett. **63**, 2540(E) (1989).

[10]M. L. Mehta, Nucl. Phys. **18**, 395 (1960); M. L. Mehta and M. Gaudin, *ibid*. **18**, 420 (1960); **22**, 340 (1961); M. Gaudin, *ibid*. **25**, 447 (1961); (reprinted in Ref. 14).

[11]M. L. Mehta, *Random Matrices and the Statistical Theory of Energy Levels* (Academic, New York, 1967).

[12]F. J. Dyson, J. Math. Phys. **3**, 166 (1962).

[13]F. J. Dyson, J. Math. Phys. **3**, 140 (1962); **3**, 1199 (1962).

[14]C. E. Porter, *Statistical Theories of Spectra: Fluctuations* (Academic, New York, 1965).

[15]J. H. Shirley, Phys. Rev. **138**, B979 (1965).

[16]K. Nakamura, Y. Okazaki, and A. R. Bishop, Phys. Rev. Lett. **57**, 5 (1986); K. Nakamura, A. R. Bishop, and A. Shudo, Phys. Rev. B **39**, 12422 (1989).

[17]K. Nakamura and H. J. Mikeska, Phys. Rev. A **35**, 5294 (1987).

[18]P. Pechukas, Phys. Rev. Lett. **51**, 943 (1983).

[19]T. Yukawa, Phys. Rev. Lett. **54**, 1883 (1985); Phys. Lett. A **116**, 227 (1986).

[20]K. Nakamura and M. Lakshmanan, Phys. Rev. Lett. **57**, 1661 (1986).

[21]J. Gibbons, T. Hermsen, and S. Wojciechowski, Phys. Lett. A **94**, 251 (1983); J. Gibbons and T. Hermsen, Physica D **11**, 337 (1984); S. Wojciechowski, Phys. Lett. **111A**, 101 (1985); Phys. Scr. **34**, 304 (1986).

[22]Infinite dynamical systems may have ergodic, mixing, or Bernoulli properties, as for the ideal gas or the harmonic solid. The global Kolmogorov-Sinai entropy per unit time is positive and infinite for these infinite systems. However, the local entropy per unit time and unit volume is zero, expressing the absence of local dynamical instability originating in the complete integrability of the corresponding finite dynamical systems. See K. L. Volkovysskii and Ya. G. Sinai, Funkts. Analiz. **5**, 19 (1971); I. P. Cornfeld, S. V. Fomin, and Ya. G. Sinai, *Ergodic Theory* (Springer-Verlag, Berlin, 1982); J. L. van Hemmen, Phys. Rep. **65**, 43 (1980); S. Goldstein, J. L. Lebowitz, and M. Aizenman, in *Dynamical Systems, Theory and Applications,* edited by J. Moser (Springer-Verlag, Berlin, 1975), p. 112. For the infinite GCM systems, such results are still conjectures.

[23]D. Fox and P. B. Kahn, Phys. Rev. **134**, B1151 (1964).

[24]H. S. Leff, J. Math. Phys. **5**, 763 (1964); Phys. Rev. **136**, A355 (1964).

[25]R. D. Kamien, H. D. Politzer, and M. B. Wise, Phys. Rev. Lett. **60**, 1995 (1988).

[26]M. L. Mehta and F. J. Dyson, J. Math. Phys. **4**, 713 (1963).

[27]F. J. Dyson, J. Math. Phys. **3**, 1191 (1962).

[28]S. Chandrasekhar, Rev. Mod. Phys. **15**, 1 (1943).

[29]M. Kuś, R. Scharf, and F. Haake, Z. Phys. B **66**, 129 (1987); F. Haake and M. Kuś, *ibid*. **6**, 579 (1988); B. Dietz and F. Haake, Europhys. Lett. **9**, 1 (1989); R. Scharf and M. Kuś, Phys. Rev. A **40**, 4774 (1989).

[30]F. J. Dyson, J. Math. Phys. **13**, 90 (1972).

[31]H. Spohn, in *Hydrodynamic Behavior and Interacting Particle Systems,* edited by G. Papanicolaou (Springer-Verlag, New York, 1987), p. 151.

[32]H. Hasegawa, H. J. Mikeska, and H. Frahm, Phys. Rev. A **38**, 395 (1988); F. Leyvraz and T. H. Seligman (unpublished).

[33]K. Nakamura and H. Thomas, Phys. Rev. Lett. **61**, 247 (1988).

[34]*Handbook of Mathematical Functions,* edited by M. Abramowitch and I. A. Stegun (Dover, New York, 1972).

[35]P. B. Kahn and C. E. Porter, Nucl. Phys. **48**, 385 (1963).